Research Article

Optimization of Microcrystalline Cellulose Production from Brewer's Spent Grain by Acid Hydrolysis

Nutcha Kongkum, Vanarat Phakeenuya and Sasithorn Kongruang*
Department of Biotechnology, Faculty of Applied Science, King Mongkut's University of Technology North Bangkok, Bangkok, Thailand

* Corresponding author. E-mail: sasithorn.k@sci.kmutnb.ac.th DOI: 10.14416/j.asep.2024.11.002
Received: 5 August 2024; Revised: 30 September 2024; Accepted: 11 October 2024; Published online: 7 November 2024

Abstract
Brewer's spent grain (BSG) is the main insoluble solid by-product of the brewing industry. To add value to this non-wood material, microcrystalline cellulose (MCC) was prepared from BSG by alkaline pretreatment, bleaching, and subsequent acid hydrolysis to produce non-wood MCC. This study aimed to optimize MCC production using a statistical design (Box-Behnken) with three factors at three levels: acid concentration (0.5–1.5 M), hydrolysis time (70–90 min) and hydrolysis temperature (55–65 °C), to achieve the maximum yield and crystallinity of MCC derived from BSG. Results from 17 experimental runs revealed that the hydrolysis condition of 0.63 M HCl for 70 min at 61 °C yielded the highest output of 15% with a crystallinity index of 60%. The chemical structures and characteristics of MCC derived from BSG were verified by Fourier transform infrared spectroscopy (FT-IR) and X-ray diffraction analysis (XRD). FT-IR analysis showed that the major wavenumbers of lignin and hemicellulose after the chemical processes (1500 cm^{-1} and 1735 cm^{-1}) decreased by 21.40% and 4.60%, respectively. The XRD chromatogram revealed that the XRD characteristic peaks were sharper after the chemical treatments, indicating an increase in cellulose crystallinity due to removing lignin and hemicellulose. The crystallinity index of MCC derived from BSG ranged from 55–64%, which is comparable in quality to commercial pharmaceutical MCC, Avicel® PH-101 (67.37%). These results demonstrated that MCC from BSG was successfully prepared by acid hydrolysis under optimized conditions. BSG proved a viable non-wood source for preparing MCC for application in the pharmaceutical and nutraceutical industries.

Keywords: Box-Behnken design, Circular economy, Fourier transform infrared spectroscopy, Microcrystalline cellulose, Scanning electron microscope, Thermogravimetric analysis

1 Introduction

Cellulose derived from non-wood biomass is used in producing biofuels, bioplastics and nanomaterials, thereby supporting a more sustainable and circular economy in food applications, pharmaceuticals and cosmetics. The non-wood plant sources of cellulose include corncob, tea waste, date seed, bamboo pulp, acacia seed, alfalfa and banana stems, as well as other plants [1]–[7], whose primary product is cellulose fiber. One of the primary by-products of the brewing industry is brewery spent grain (BSG), considered as the most interesting non-wood source for extracting both cellulose and cellulose derivatives. BSG is a fibrous byproduct primarily consisting of cellulose, hemicellulose and lignin. It is abundant in proteins, fermentable sugars and bioactive compounds. These properties make BSG a valuable feedstock for producing a variety of high-value products. While it is commonly used as animal feed, its potential for other applications such as food additives (thickener, stabilizer and emulsifier), fuel (biogas production) and pharmaceutical applications (filler, binder, and disintegrant) has sparked considerable interest. Additionally, this biomaterial is readily available at low cost throughout the year and is produced in large quantities by industrial breweries. This residue accounts for approximately 85% of the total by-products generated [8]. On average, spent grains comprise 20–31% of the original malt weight, equating to roughly

20 kg (wet weight) per 100 L of beer produced [9]. The composition of BSG varies but is primarily made up of hemicellulose, in the form of arabinoxylans and cellulose. Hemicellulose content ranges from 19–40%, while cellulose content varies between 9–25% per dry matter [10]–[12]. The benefits of utilizing non-wood lignocellulose biomass as a cellulose source include its low cost, widespread availability, abundance and the reduction of waste that would otherwise be disposed of through low-value animal feed.

The extraction of cellulose from lignocellulosic biomass can involve different processes depending on the biomass source, production type and desired cellulose quality. Various methods for extracting cellulose from lignocellulosic biomass, such as acid or alkaline pulping [13], [14], steam-explosion [15]–[17], organosolv [18]–[20], neutral deep eutectic solvent and Lewis base [21]–[23], ionic liquid [24]–[26], supercritical fluid with alkaline extraction [27]–[29] and enzymatic hydrolysis [30]–[32] have been extensively researched. When compared for feasibility analysis, acid and alkaline pulping with the chosen bleaching chemical and technique prevail over the rest of the aforementioned processes.

Microcrystalline cellulose (MCC) is a refined, crystalline powder, partially depolymerized polymer with numerous industrial applications. Common commercial methods for producing MCC involve the partial acid hydrolysis of purified cellulose. During this process, only the amorphous regions of the polysaccharides are hydrolyzed, dissolved, and removed, while the crystalline cellulose regions remain intact and can be recovered. The acid hydrolysis process is typically considered complete once a specific degree of polymerization is achieved. Extracting cellulose from non-wood sources demands less chemical and energy consumption due to their relatively low lignin contents compared to wood, which typically contains high lignin and requires more chemicals and energy [33]–[35]. A previous study on acid hydrolysis for cellulose-derived BSG production by Mussatto *et al*., [36] reported only on the specific method of using a sulfuric acid solution to treat BSG with a solid-to-liquid ratio of 1:8 g/g at 120 °C for 17 min to delignify and remove hemicellulose. Although many reports have been published on MCC production using strong acid hydrolysis, such as HCl, H_2SO_4, and HNO_3, most of these studies focused on other lignocellulosic materials (e.g., tea waste, date seeds, Bambara nuts, corncobs, bamboo pulp, cottonwood, corn husks, and rice husks) with specific acid concentrations, fixed temperatures and hydrolysis times under varying solid-to-liquid ratios [1]–[4], [37]–[41]. However, the optimization process via acid hydrolysis after alkaline treatment for MCC production from brewery spent grain (BSG) has not been reported. Several other factors significantly affect the acid hydrolysis process for producing MCC, including solid-to-liquid ratio (solid loading), type of acid, lignocellulosic source, pretreatment method, and mixing and agitation during hydrolysis [2], [4], [42]. A significant factor affecting acid hydrolysis for the production of MCC is acid concentration. The concentration of the acid directly influences the degree of hydrolysis, which in turn affects the yield, particle size, crystallinity, and purity of the resulting MCC [2], [4], [43]. Moreover, both temperature and time of hydrolysis are critical factors in acid hydrolysis for the production of MCC [2], [4], [44]. Higher temperatures accelerate the hydrolysis reaction, promoting the breakdown of amorphous cellulose regions into microcrystalline forms. However, excessive temperatures can lead to over-hydrolysis, causing degradation of the cellulose, reducing its quality and possibly forming unwanted by-products. For the MCC production process, the duration of hydrolysis plays a key role in determining the extent of cellulose breakdown. Shorter hydrolysis times may result in incomplete conversion to MCC, while longer times can increase the degree of hydrolysis [45]–[47]. Consequently, the aim of this study was to optimize MCC production using Box-Behnken Design and to characterize the BSG-derived MCC before and after chemical treatments using scanning electron microscopy (SEM). Additionally, X-ray diffraction (XRD), Fourier-transform infrared spectroscopy (FTIR), and thermal properties via thermogravimetric analysis were examined. The operational production methods resulting from the optimized case study were also reported.

2 Materials and Methods

2.1 *Chemicals*

Brewer's spent grain (BSG) was supplied from a commercial brewery in Nakorn Pathom, Thailand. Commercial microcrystalline cellulose, Avicel® PH-101 was purchased from Sigma-Aldrich Chemicals (Madrid, Spain). Sodium hydroxide and hydrogen peroxide (30–32%) were bought from ANaPURE (New Zealand). Hydrochloric acid (37%) was obtained from QRëC (New Zealand). Sodium hypochlorite (10%) was purchased from LOBA Chemie (Mumbai, India). All reagents were of analytical grade.

2.2 *Brewer's spent grain preparation*

The BSG residues were taken from lautering from the brewing process. BSG was dried with an oven dryer at 75 °C for 24 h with periodic flipping over every 4 h to achieve a moisture content of less than 8%. The dried brewer's spent grain was pulverized and passed through 70 mesh size sieve shakers to get a brewer's spent grain powder.

2.3 *Extraction of cellulose from brewer's spent grain*

Triplicate alkaline pretreatments were performed in a 250 mL Erlenmeyer flask by treating brewer's spent grain powder 10 g with 100 mL of 1.5 M sodium hydroxide solution. The reaction was run at 80 °C for 90 min. The pellet was collected from alkaline pretreatment and then was bleached with 5% v/v sodium hypochlorite and hydrogen peroxide for 20 min at 80 °C. The pellet was collected after the centrifugation. The bleaching was applied by adding 10 %v/v NaOCl at 70 °C for 20 min before subjected to centrifugation to separate the precipitate. The white slurry of the precipitated part was cleaned with 100 mL of distilled water before centrifugation. The collected pellet was then dried with a freeze dryer.

2.4 *Optimization of acid hydrolysis condition for microcrystalline cellulose production*

Response surface methodology (RSM) was employed to optimize the acid hydrolysis conditions using Box-Behnken design (BBD). The mathematical model considered three factors at three levels for optimization: acid concentration (0.5, 1, 1.5 M), hydrolysis temperature (55, 60, 65 °C), and hydrolysis time (70, 80, 90 min), as shown in Table 1.

Cellulose extracted from brewer's spent grain was treated with different concentrations of hydrochloric acid to produce microcrystalline cellulose based on the experimental design. MCC yield and crystallinity index were explained by the quadratic model in Equation (1).

$$y = \beta_0 + \sum_{i=1}^{n} \beta_i X_i + \sum_{i=1}^{n-1} \sum_{j=2}^{n} \beta i_j X_i X_j + \sum_{i=1}^{n} \beta i_j X_i^2 \qquad (1)$$

Table 1: Process variable and level of Box-Behnken Design.

Factor	Level			Unit
	–1	0	1	
Acid concentration	0.5	1.0	1.5	mol/L
Temperature	55	60	65	°C
Time	70	80	90	min

This model was used to quantify the relationships between the estimated responses (yield (g), y_1, and crystallinity index (%), y_2) and the three independent variables (X_i and X_j: acid concentration, hydrolysis temperature, and hydrolysis time). The β values were coefficients obtained through multiple regression analysis. These coefficients quantify the significance of linear effects, quadratic effects, and interactions between factors. Regression analysis and analysis of variance (ANOVA) were conducted, with *p*-values less than 0.05 being considered statistically significant. Significant differences among pretreatments in relation to MCC components derived from BSG, including yield and crystallinity, were analyzed using multiple regression and Fisher's least significant difference test. All statistical analyses were performed using Design-Expert software version 13 (Stat-Ease Inc., USA). The selected quadratic model was used as the mathematical equation to evaluate the optimization conditions. The optimal acid hydrolysis conditions were determined to maximize the yield and crystallinity index of microcrystalline cellulose. The number of experimental runs is presented in Table 2.

Table 2: Box-Behnken for three independent variables and responses for MCC derived BSG production.

Run	Variables			Responses	
	Acid conc. (mol/L)	Tempt. (°C)	Time (min)	Yield (g)	CrI (%)
1	1.5	65	80	1.06	59.03
2	0.5	65	80	1.52	54.51
3	0.5	60	70	1.68	59.07
4	1.5	60	70	1.10	58.90
5	0.5	60	90	1.09	57.58
6	1.5	60	90	1.34	58.30
7	0.5	55	80	1.11	59.72
8	1.5	55	80	1.03	58.28
9	1	60	80	1.08	62.63
10	1	60	80	1.09	59.78
11	1	60	80	1.18	63.46
12	1	60	80	1.23	61.02
13	1	60	80	1.10	61.35
14	1	55	90	1.06	60.42
15	1	55	90	1.01	62.05
16	1	65	70	1.05	62.77
17	1	55	70	0.94	60.62

2.5 *Validation and case study of optimization criteria*

MCC was prepared from BSG using the optimum conditions determined in Section 2.4. The experiment was conducted in triplicate to validate the yield and crystallinity index. To evaluate operational criteria, five different sets of MCC production conditions were analyzed by response surface methodology. These conditions aimed to find alternative operational settings to maximize both yield and crystallinity: Case I included all factors within defined ranges; Case II set acid concentration at its lowest while maintaining hydrolysis time and temperature within specified ranges; Case III set hydrolysis temperature at its lowest, with hydrolysis time and acid concentration within specified ranges; Case IV set hydrolysis time at its lowest, with hydrolysis temperature and acid concentration within specified ranges; and Case V set all factors at their lowest values.

2.6 *Characterization of BSG, MCC derived BSG and Avicel® PH-101*

2.6.1 Fourier transform infrared spectroscopy

The pulverized and dried samples (10 mg) were mixed with potassium bromide (200 mg) followed by grinding to a fine powder before compressing into tablets. Then analysis was performed by the Fourier Transform Infrared Spectroscopy (INVENIO S, BRUKER, Germany) by scanning with an average of 25 scans in the range of 4000–400 cm^{-1} at a spectral resolution of 2 cm^{-1}.

2.6.2 X-ray diffraction (XRD)

XRD patterns were obtained using an X-ray diffractometer (SmartLab, Rigaku, Japan) with Cu Kα radiation for observing the crystalline nature of the untreated BSG with MCC derived BSG and the Avicel® PH-101. The sample was scanned in a 2θ range from 5° to 40°. Values of crystallinity were recorded from the ratio between the intensity of the (002) peak and the (101) peak. The crystallinity indexes (CrI) of the sample were calculated using the following equation.

$$\% \text{ Crystallinity Index (CrI)} = \frac{(I_{002} - I_{am})}{I_{002}} \; x \; 100$$

When I_{002} is the maximum diffraction intensity of crystalline from a plane (002) at 2θ = 22.2°
I_{am} is s the intensity of amorphous cellulose at 2θ = 18°

2.6.3 Thermogravimetric (TGA)

The characterization of thermal analysis of samples before and after chemical pretreatment was performed using the Thermogravimetric analyzer (PerkinElmer, TGA 4000, USA) with a heating rate of 10 °C/min and a temperature range of from 25 °C – 950 °C under nitrogen atmosphere.

2.6.4 Scanning electron microscopy (SEM)

The morphological characteristics of changes in samples due to pretreatment were observed by SEM. For the sample preparation, the BSG, BSG derived MCC and Avicel® PH-101 were fixed on stubs and coated with Auto fine coater (JEC-3000FC). A field emission scanning electron microscope (FESEM, JSM-7610FPlus, JEOL, Japan) with an accelerating voltage of 3.0 kV up to 5.0 kV was operated. The SEM images of three samples at various magnifications, 750x, 3500x and 1000x were recorded.

2.6.5 Statistical analysis

All the analytical experiments were carried out in triplicate. The results were compared by ANOVA using the SPSS 9.0. Multiple comparison of the means was performed by the Least Significant Difference (LSD) test at a 0.05 level.

3 Results and Discussion

3.1 *Optimization of MCC derived BSG production*

In the process of producing BSG-derived MCC, alkaline treatment was applied to purify the cellulose from BSG by removing residual hemicellulose, lignin, and other remaining impurities. During this alkaline treatment, the cellulose chains in the treated BSG were reduced in size, resulting in more crystalline segments. After that, bleaching with NaOCl was used to effectively remove colored impurities and residual lignin, resulting in a white product. Furthermore, the treated BSG was subjected to H_2O_2 to neutralize any residual NaOCl, ensuring that the MCC would be free from bleaching agents that could affect its properties. This production step was crucial for achieving high purity and quality of the final MCC product.

To produce BSG-derived MCC, potential influencing factors for MCC parameters during the acid hydrolysis of BSG were optimized using response surface methodology (RSM) to ensure maximum yield

and crystallinity. The results of 17 experiments detailing the yield and crystallinity index from the Box-Behnken Design are presented in Table 2. The experimental data were fitted to a quadratic equation, which depicted the relationship between the various parameters used in the model. The quadratic equation for production yield had an R^2 value of 89.10 and an adjusted R^2 value of 96.50, indicating a good fit of the model to the data. The model's F-value of 6.38, along with a *p*-value of less than 0.05, confirmed its statistical significance. The statistical evaluation showed that the yield of microcrystalline cellulose (MCC) was significantly influenced by acid concentration (*p*-value = 0.0138). Furthermore, during production involving alkalization, bleaching, and acid hydrolysis, the yield of MCC was notably affected by the synergistic interaction between acid concentration and hydrolysis time (*p*-value = 0.0034).

The MCC yield averaged approximately 10% of the original BSG material, with a crystallinity index ranging from 54% to 63%, as detailed in Table 2. Three-dimensional response plots (Figure 1(a)–(c) and Figure 2(a)–(c)) were generated to understand the interactions between different variables and determine the optimal levels for maximum response. These plots provided valuable insights into the interactions among the factors tested. The contour plots indicated significant interactions between the parameters considered in this study. The effects of hydrolysis time and acid concentration are shown in Figure 2(b), while Figure 2(c) depicts the response surface representing changes in hydrolysis time and temperature and their impact on yield. The peak points on the three-dimensional plots revealed the optimal conditions for achieving maximum MCC yield from BSG. Each response model underwent statistical analysis via ANOVA to confirm its reliability. Temperature changes outside the range of 60°C did not significantly affect MCC yield. This consideration is reflected in the production results of MCC derived from BSG, illustrated in Figure 2(a). The results showed that lower acid concentrations combined with higher hydrolysis temperatures led to increased MCC yields, ranging from 1.11 g to 1.52 g. The maximum yield observed was 1.52 g, with an HCl concentration of 0.63 M at 61 °C and a hydrolysis time of 70 min, resulting in a crystallinity index of 60%. Figure 2(a) illustrates the effect of acid concentration and temperature on MCC yield, with hydrolysis time held constant. The concentration of HCl directly influenced the degree of hydrolysis, which in turn affected the yield, particle size, crystallinity index and purity of the resulting MCC. Although higher acid concentrations typically led to more extensive hydrolysis, effectively breaking down the amorphous regions of cellulose, excessive concentrations could cause cellulose degradation, reducing the quality of the MCC. In contrast to the MCC yield under acid hydrolysis conditions, the ANOVA analysis for the effect of crystallinity index on MCC yield indicated an F-value of 2.71 with a *p*-value greater than 0.05, suggesting that the model was not significant in predicting changes in the crystallinity index. In this experiment, the acid concentration range tested was from 0.5 to 1.5 mol/L, which is still considered a moderate condition for acid hydrolysis treatment. Therefore, during acid hydrolysis due to the inherent structure and composition of the cellulose in the region. During acid hydrolysis, the amorphous cellulose in BSG was more easily degraded, while the crystalline cellulose remained largely intact, even at higher acid concentrations. However, the model adequately predicted changes in the crystallinity index with a coefficient of determination (R^2) value of 0.776, considering the relationships among acid concentration, temperature, and hydrolysis time. These relationships are illustrated in the response surface graphs in Figures 1(a)–(c). The model predicted optimal acid hydrolysis conditions at 61 °C for 70 min with an acid concentration of 0.635 M. These parameters maximized the yield to 15.18% (1.518 g) with a crystallinity index of 60. Equations for yield and crystallinity index are provided below.

$$\textbf{Yield (g)} = -18.84 - 2.6A + 0.7B + 0.005C - 0.0374AB + 0.0411AC - 0.0008BC + 0.667A^2 - 0.0048B^2 + 7.5C^2 \quad (2)$$

$$\textbf{Crystallinity Index (\%)} = 35.76 - 11.34A + 1.43B - 0.24C + 0.60AB + 0.04AC - 0.002BC - 13.53A2 - 0.01B^2 + 0.01C^2 \quad (3)$$

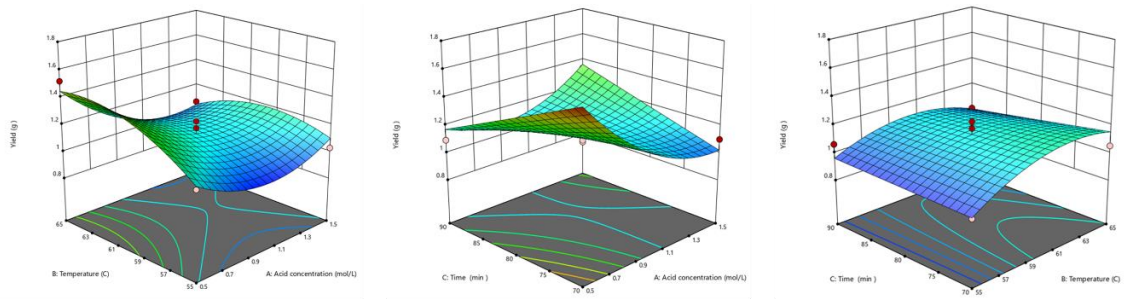

(a) (b) (c)

Figure 1: Response surface 3D graph of yield in MCC production (a) the effect of acid concentration and temperature, (b) the effect of acid concentration and hydrolysis time, (c) hydrolysis temperature and time.

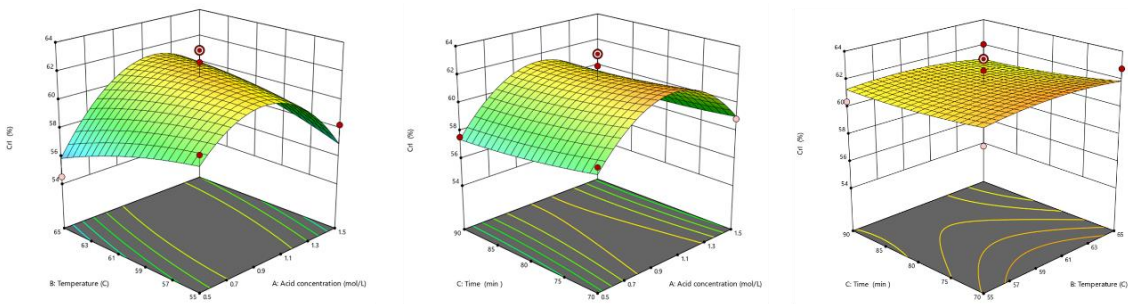

(a) (b) (c)

Figure 2: Response surface 3D graph of crystallinity index in MCC production (a) the effect of acid concentration and temperature, (b) the effect of acid concentration and hydrolysis time, (c) hydrolysis temperature and time.

The acid hydrolysis treatment of BSG resulted in a white, fibrous powder composed of porous particles from the brownish ground particle of BSG, as shown in Figure 3.

Figure 3: Appearance of MCC derived BSG from acid hydrolysis production.

3.2 *Characterization of microcrystalline cellulose*

FTIR spectroscopy was utilized to identify functional groups and chemical changes occurring during the pretreatment process. Graphs of FTIR spectra of BSG, MCC derived from BSG, and Avicel® PH-101 were presented in Figure 4. In its raw form, BSG powder exhibited seven notable peaks in the spectra at 1029 cm^{-1}, 1525 cm^{-1}, 1633 cm^{-1}, 1735 cm^{-1}, 2856 cm^{-1}, 2921 cm^{-1} and 3284 cm^{-1}. The transmittance peak at 1029 cm^{-1} indicated dominant cellulose (C6-O6H stretching) and lignin (C–O stretching). Following alkaline, bleaching with NaOCl and H_2O_2 and acid hydrolysis treatments, this peak sharpened, reflecting structural changes. The peak at 1525 cm^{-1}, attributed to various lignin groups, notably diminished post-alkaline and bleaching treatments, suggesting the removal of hemicelluloses and lignin from BSG. Comparative analysis showed increases of 5.64%, 2.67%, 21.4%, and 4.6% in transmittance at main lignin and hemicellulose wavenumbers (2900 cm^{-1}, 2800 cm^{-1}, 1500 cm^{-1} and 1735 cm^{-1}), as depicted in Figure 4. The prominent peak at 1635 cm^{-1}, associated with alkenyl C=C stretching and aromatic skeletal C=C vibration in lignin, increased by 12.37% and 7.64%, respectively, following bleaching stages. Absence of these peaks in MCC derived from BSG indicated effective removal of hemicellulose and lignin components during treatment. Our result of delignification and hemicellulose removal at this peak was similar to the previous investigation by Sheng *et al.* [37], Shao *et al.* [1], Asif *et al.*, [48]. They showed that

the wavelengths that represented lignin and hemicellulose were decreased after the chemical pretreatment of cotton wool, corncob and dated seed. The peak at 1735 cm^{-1}, attributed to C=O stretching in acetyl groups of hemicellulose, appeared weaker in both MCC derived from BSG and Avicel® PH-101, suggesting reduced acetyl groups post-treatment. Changes in peak intensity indicated acetyl group disappearance during pretreatment.

Table 3: Assignment of key functional groups associated with lignocellulosic material.

Wavenumber (cm^{-1})	Functional Group Assignment	Reference
3500 – 3200	–OH bond in cellulose, hemicellulose and lignin	[49] – [51]
2896 – 2922	Symmetric methyl and methylene stretching of cellulose, hemicellulose and lignin	[51], [52]
1735	C=O stretching in the carboxyl and ester bonds of hemicellulose	[49] – [53]
1640	C=C of aromatic vibrations in lignin	[53], [54]
1500 – 1525	C=C in the aromatic ring of Guaiacyl unit of lignin	[52], [53]
1240	C-O bond in hemicellulose and lignin (syringyl aromatic ring)	[53], [55]
1029 – 1031	C–O–C of pyranose ring skeletal vibration	[48]
897	C–H rocking vibration of beta-glycosidic linkage	[49], [50], [55]

The prominent bands observed in all samples in the FT-IR spectra ranging from 3000 to 3500 cm^{-1} were assigned to OH stretching vibrations, indicating the presence of cellulose in the samples. Within the cellulose structure, three hydroxyl groups typically interact with others to form secondary valence bonds, which contribute to cellulose crystallinity and chain structure through a hydrogen bonding network. The increased intensity of these bands suggested that the pretreatment effectively degraded the amorphous parts, enhancing the crystallinity of MCC derived from BSG. Specifically, peaks at 3300 cm^{-1}, 1025 cm^{-1} and 897 cm^{-1} were assigned to -OH groups of the sugar ring, pyranose sugar ring and β-glycosidic linkages, respectively. The heightened intensity of these peaks indicates successful extraction resulting in a higher cellulose content. Overall, the spectral profiles of the final acid-treated BSG displayed typical absorption peaks of cellulose, akin to those observed in commercially available Avicel® PH-101, featuring main peaks at 3345 cm^{-1}, 2898 cm^{-1}, and 1027 cm^{-1}. The peak at 2898 cm^{-1} in acid-treated, bleached BSG and 2893 cm^{-1} in Avicel® PH-101 indicates C–H stretching. Additionally, the absorption peak at 895 cm^{-1} corresponds to –C–H out-of-plane stretching in the cellulose position ring due to β-linkages [56], which was observed at 898 cm^{-1} in MCC derived from BSG. Details of the major wavelength of agricultural biomass were classified in Table 3. These findings highlight the similarity in cellulose composition between MCC from BSG and Avicel® PH-101, affirming the efficacy of the extraction and refining processes in producing high-quality MCC from BSG.

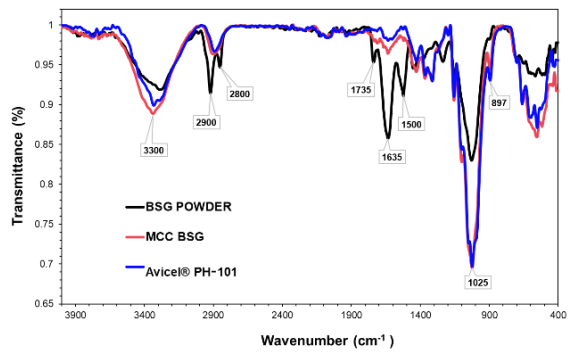

Figure 4: Comparison of FTIR spectra of BSG, MCC derived BSG, Avicel® PH-101.

3.1.2 X-ray diffraction analysis

X-ray diffraction patterns for MCC-derived BSG and the standard Avicel® PH-101 were depicted in Figure 5. Generally, components of lignocellulosic biomass can be either crystalline or amorphous. Cellulose contributes to the crystalline structure, whereas hemicellulose and lignin are typically amorphous [57]. During acid hydrolysis, an increase in crystallinity was anticipated, as evidenced by the XRD curve. Thus, heightened crystallinity showed greater cellulose content and reflected the efficacy of the pretreatment process. Native cellulose, known as Cellulose I, exhibited characteristic peaks at 2θ values of 15°, 16°, and 23°, corresponding to the 100, 110, and 002 reflections, respectively. In contrast, mercerized and regenerated cellulose, categorized as Cellulose II, showed typical peaks at approximately 12°, 20°, and 22° for the same reflections [58]. As shown in Figure 5, the two materials displayed slightly different X-ray diffraction patterns, likely due to variations in the source of the MCC. MCC-derived BSG and Avicel® PH-101 exhibited diffraction patterns with peaks at 2θ = 15.6°, 22.2°, and 35°, corresponding to the 110, 200, and 004 crystallographic

planes, respectively, indicative of the typical crystalline structure of cellulose I. Avicel® PH-101 was traditionally characterized by a high degree of crystallinity, typically ranging between 55–80% as determined by X-ray diffraction spectroscopy [38]. Our diffraction pattern along with crystallographic planes from MCC derived BSG was according to the previous studies by Sheng *et al*. [37], Zhang *et al*. [4], and Shao *et al*. [1], which produce MCC derived from cotton wool, corncob and corncob.

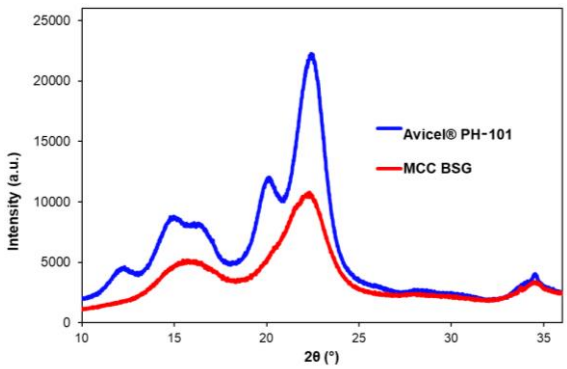

Figure 5: XRD chromatogram of MCC derived BSG and Avicel® PH-101.

3.1.3 Thermogravimetric analysis

TGA of BSG, MCC-derived BSG, and Avicel® PH-101 were illustrated in Figure 6. Thermal decomposition of the samples was investigated via TGA from 25 °C to 900 °C at 10 °C/min under a nitrogen atmosphere. Analysis of the TG curve (Figure 6) for BSG showed an initial thermal event between 25–48 °C and 122–268 °C, with observed weight losses of about 6.79% and 25.59%, attributed to water evaporation. The final thermal degradation occurred between 324–343 °C, resulting in a weight loss of 42.44%. This observation was supported by moisture content determination. For MCC-derived BSG, the first thermal degradation was between 25–38 °C, resulting in a weight loss of 5.09%. Similarly, the Avicel® PH-101 sample showed an initial thermal event for water evaporation between 25–47 °C, with a weight loss of 5.30%. The second thermal event for MCC-derived BSG occurred between 280–310 °C, resulting in approximately 94.54% weight loss. For Avicel® PH-101, the second thermal event occurred between 310–334 °C, with a weight loss of 92.12%. All samples showed rapid pyrolysis between 280 °C and 350 °C, with weight losses primarily due to dehydration and cellulose decomposition. The maximum weight losses for BSG, MCC-derived BSG and Avicel® PH-101 were observed at 343.10 °C, 310.82 °C, and 334.73°C, respectively. The maximum weight loss temperature of MCC derived BSG was similarly to the maximum weight loss temperature of MCC derived from alfalfa [6] and acacia seed [5] which were 320 °C and 304 °C. The thermal weight loss observed between 200–400 °C was attributed to cellulose depolymerization [58]. Results indicated that MCC-derived BSG exhibits thermal stability comparable to Avicel® PH-101. This high thermal stability suggested the potential applications in food, pharmaceuticals and green composite products.

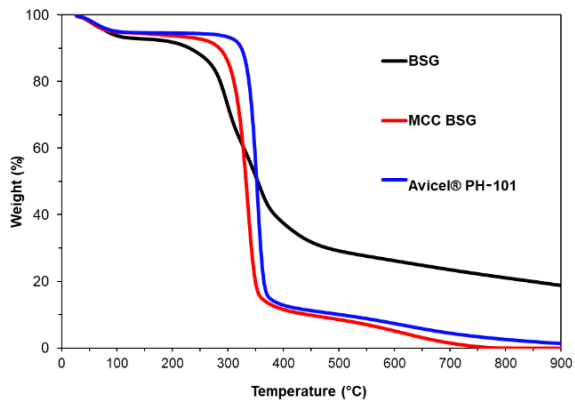

Figure 6: TGA curves of BSG, MCC derived BSG and Avicel® PH-101.

3.1.4 Scanning electron microscope

Scanning electron microscope (SEM) images were used to assess the effect of chemical treatment on BSG, MCC-derived BSG, and Avicel® PH-101, as shown in Figure 7. The results indicated that raw BSG exhibits a rough surface, likely due to the presence of hemicellulose and lignin deposits. Following the pretreatment procedure, MCC-derived BSG showed elongated fibrillar shapes with a smoother surface compared to raw BSG. The production of MCC from BSG resulted in smoother cellulose fibrils predominantly in a rod-like structure. In contrast, the commercial standard microcrystalline cellulose, Avicel® PH-101, exhibited shorter rod-like structures and some agglomerated fibril pieces, as observed in the 750x magnification. As depicted in Figure 7, the surface morphology of our MCC-derived BSG was found to be comparable to that of Avicel® PH-101. This similarity in morphology confirmed the successful removal of hemicellulose and lignin originally bonded to the surface of the ground BSG.

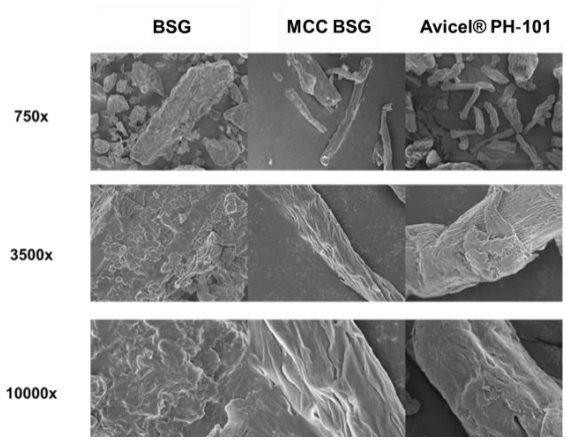

Figure 7: SEM micrograph image of BSG, MCC derived BSG and Avicel® PH-101 at 750x, 3500x, and 10000x.

3.3 *MCC derived BSG acid hydrolysis process validation*

The operational conditions for acid hydrolysis were validated using a 0.634 M HCl concentration at 61 °C for 70 min, resulting in a maximum yield of 1.518 g of MCC. This validated operational condition and the accuracy of the yield mathematical equation were tested in triplicate. Each replication showed yields approximately 10% slightly higher than the predicted yield in the model, as shown in Table 4. These experimental results were in good agreement with the predictions of the quadratic regression model. For MCC derived from BSG, our operational conditions were simpler to handle than those previously reported by Heidari *et al*., [59], BSG was initially treated with a 2 wt.% sodium hydroxide aqueous solution for 2 hours at 80 °C under gentle agitation. The alkaline-treated BSG underwent bleaching with 1.7 wt.% sodium chlorite and acetate buffer for 2 hours at 80 °C under gentle agitation. This was followed by micro-fluidization with and without 2,2,6,6-Tetramethylpiperidine-1-oxyl radical (TEMPO)-mediated oxidation pretreatment to obtain bio-based building blocks for aerogels. The lower temperature of acid hydrolysis and shorter hydrolysis time from our results made it more economical to scale up compared to the report from Camacho-Núñez *et al*., [60] that extracted cellulose from BSG through acid hydrolysis, alkaline hydrolysis and bleaching reactions. BSG was first treated with HNO_3 at a concentration of 6% (w/v) at 80 °C for 60 min, followed by alkaline hydrolysis with 2% (w/v) NaOH at 80 °C for 90 min. The cellulose was then purified via a one-step bleaching reaction with a 5% (v/v) H_2O_2 aqueous solution at 70 °C for 60 min. Additionally, Bhandari *et al*., [61] prepared microcrystalline cellulose from rice husk through alkaline pretreatment with 10% w/v sodium hydroxide at 55 °C for 90 min. The sodium hydroxide-treated material underwent further processing in the presence of 0.5%–1% sodium chlorite at 85 °C for 90 min, followed by acid hydrolysis with 2.5N hydrochloric acid and hydrogen peroxide treatment, resulting in a yield of 5 g of MCC from 20 g of rice husk.

3.4 *The alternative operational condition for production*

For this research, the acid hydrolysis operational parameters were confirmed by employing a 0.634 M HCl solution at 61 °C for 70 min, yielding a maximum of 1.518 g of MCC. To produce MCC from BSG under constrained conditions and considering techno-economic analysis, various parameters for acid hydrolysis extraction were evaluated and tabulated in Table 5. In order to minimize hydrolysis time and reduce costs associated with acid and electricity (taking temperature into account), Case V emerged as the optimal condition. Under Case V, a yield of 1.438 g of MCC with a crystallinity index of 59.47% was achieved using 0.5 M acid hydrolysis at 56.30 °C for 70 min. Among the 17 experimental runs tested for acid concentration and hydrolysis temperature, Case III closely matched the conditions of Case V. Treatment of BSG with 0.507 M acid at 56 °C for 70 min in Case III yielded 1.434 g of MCC with a 59% crystallinity index.

Table 4: Validation of yield and crystallinity index.

Response	Validation Experiments			$\bar{x}$	SD
	1	2	3		
Yield (g)	1.0	1.02	1.00	1.02	0.01
Crystallinity Index (CrI)	56.7	57.6	55.5	56.6	0.84

Table 5: Case study of MCC production process.

Case	Condition			Desired Response		Optimum Condition		
	[HCl] (mol/L)	Temp. (C)	Time (min)	Yield (g)	CrI (%)	[HCl] (mol/L)	Temp. (C)	Time (min)
Case I	In range	In range	In range	1.518	60	0.634	61	70
Case II	Lowest (0.5M)	In range	In range	1.609	59	0.530	59.89	70
Case III	In range	Lowest (55C)	In range	1.434	59	0.507	56.36	70
Case IV	In range	In range	Lowest (70 min)	1.518	60	0.634	61	70
Case V	Lowest	Lowest	Lowest	1.438	59.47	0.500	56.30	70

4 Conclusions

We optimized the production of MCC from BSG through pretreatment followed by acid hydrolysis. The optimal conditions for MCC production involved acid hydrolysis using 0.634 M HCl at 61°C for 70 minutes, achieving a maximum yield of 67% and crystallinity of 57%. For the MCC production process, the higher temperature and longer hydrolysis time would be possible to achieve a higher yield. However, the cost of the production process has to be considered. The yield of MCC was significantly influenced by acid concentration and the interaction between acid concentration and hydrolysis time during the alkalization, bleaching, and acid hydrolysis processes. Scanning electron microscopy revealed the morphological characteristics of the produced MCC derived from BSG. Thermal properties were analyzed using thermogravimetric analysis (TGA), focusing on key properties such as crystallinity. Our findings demonstrate successful production of MCC from BSG, readily to apply the condition for scaling up process, although further exploration of its physicochemical characteristics and applications is warranted.

Acknowledgments

This study was supported by grant from Work-integrated Learning Project (WiL) by National Science Technology and Innovation Policy Office and Department of Biotechnology, Faculty of Applied Science, KMUTNB for their facilities support.

Author Contributions

N.K.: conceptualization, data curation, data analysis formal analysis, methodology, research design, writing an original draft; V.P.: investigation, writing—reviewing and editing; S.K.: conceptualization, data curation, writing—reviewing and editing, funding acquisition, project administration. All authors have read and agreed to the published version of the manuscript.

Conflicts of Interest

The authors declare no conflict of interest.

References

[1] X. Shao, J. Wang, Z. Liu, N. Hu, M. Liu, and Y. Xu, "Preparation and characterization of porous microcrystalline cellulose from corncob," *Industrial Crops and Products*, vol. 151, Sep. 2020, Art. no. 112457, doi: 10.1016/j.indcrop.2020.112457.

[2] T. Zhao, Z. Chen, X. Lin, Z. Ren, B. Li, and Y. Zhang, "Preparation and characterization of microcrystalline cellulose (MCC) from tea waste," *Carbohydrate Polymers*, vol. 184, pp. 164–170, Mar. 2018, doi: 10.1016/j.carbpol.2017.12.024.

[3] N. Y. Abu-Thabit, A. A. Judeh, A. S. Hakeem, A. Ul-Hamid, Y. Umar, and A. Ahmad, "Isolation and characterization of microcrystalline cellulose from date seeds (*Phoenix dactylifera* L.)," *International Journal of Biological Macromolecules*, vol. 155, pp. 730–739, Jul. 2020, doi: 10.1016/j.ijbiomac.2020.03.255.

[4] Y. Zhang, Y. Xu, X. Yue, L. Dai, and Y. Ni, "Isolation and characterization of microcrystalline cellulose from bamboo pulp through extremely low acid hydrolysis," *Journal of Wood Chemistry and Technology*, vol. 39, no. 4, pp. 242–254, Apr. 2019, doi: 10.1080/02773813.2019.1566365.

[5] M. Husin, A. R. Li, N. Ramli, A. Z. Romli, M. I. Hakimi, and Z. Ilham, "Preparation and characterization of cellulose and microcrystalline cellulose isolated from waste Leucaena leucocephala seeds," *International Journal of*

Advanced and Applied Sciences, vol. 4, no. 3, pp. 51–58, Mar. 2017, doi: 10.21833/ijaas.2017.03.009.

[6] Z. Bahreini, M. Abedi, and D. S. Fateh, "A study on preparation and characterization of microcrystalline cellulose from Lucerne (alfalfa) waste fibers," *Research Square (Research Square)*, Jul. 2022, doi: 10.21203/rs.3.rs-1529185/v1.

[7] V. Suchiya, P. Potiyarj, and D. Aht-Ong, "Preparation and characterization of microcrystalline cellulose from cellulose based-agro wastes," *Journal of Engineering and Applied Sciences*, Jul. 2022, doi: 10.3923/jeasci.2016.2566.2572

[8] M. P. Fernández, J. F. Rodriguez, M. T. García, A. De Lucas, and I. Gracia, "Application of supercritical fluid extraction to brewer's spent grain management," *Industrial & Engineering Chemistry Research*, vol. 47, no. 5, pp. 1614–1619, Jan. 2008, doi: 10.1021/ie0708529.

[9] S. I. Mussatto, G. Dragone, and I. C. Roberto, "Brewers' spent grain: Generation, characteristics and potential applications," *Journal of Cereal Science*, vol. 43, no. 1, pp. 1–14, Jan. 2006, doi: 10.1016/j.jcs.2005.06.001.

[10] C. Xiros, E. Topakas, P. Katapodis, and P. Christakopoulos, "Hydrolysis and fermentation of brewer's spent grain by *Neurospora crassa*," *Bioresource Technology*, vol. 99, no. 13, pp. 5427–5435, Sep. 2008, doi: 10.1016/j.biortech.2007.11.010.

[11] P. E. Plaza, L. J. Gallego-Morales, M. Peñuela-Vásquez, S. Lucas, M. T. García-Cubero, and M. Coca, "Biobutanol production from brewer's spent grain hydrolysates by *Clostridium beijerinckii*," *Bioresource Technology*, vol. 244, pp. 166–174, Nov. 2017, doi: 10.1016/j.biortech.2017.07.139.

[12] M. Parchami, J. A. Ferreira, and M. J. Taherzadeh, "Brewing process development by integration of edible filamentous fungi to upgrade the quality of brewer's spent grain (BSG)," *BioResources*, vol. 16, no. 1, pp. 1686–1701, Jan. 2021, doi: 10.15376/biores.16.1.1686-1701.

[13] Y. Pu, N. Jiang, and A. J. Ragauskas, "Ionic liquid as a green solvent for lignin," *Journal of Wood Chemistry and Technology*, vol. 27, no. 1, pp. 23–33, Apr. 2007, doi: 10.1080/02773810701282330.

[14] F. S. Toma, Z. Jemaat, M. D. H. Beg, M. R. Khan, and R. M. Yunus, "Comparison between lignin extraction by alkaline and ultrasound-assisted alkaline treatment from oil palm empty fruit bunch," *IOP Conference Series Materials Science and Engineering*, vol. 1092, no. 1, Mar. 2021, Art. no. 012027, doi: 10.1088/1757-899x/1092/1/012027.

[15] V. M. Serrano-Martínez, H. Pérez-Aguilar, M. P. Carbonell-Blasco, F. Arán-Ais, and E. Orgilés-Calpena, "Steam explosion-based method for the extraction of cellulose and lignin from rice straw waste," *Applied Sciences*, vol. 14, no. 5, Mar. 2024, Art. no. 2059, doi: 10.3390/app14052059.

[16] M. A. Pérez-Limiñana, H. Pérez-Aguilar, C. Ruzafa-Silvestre, E. Orgilés-Calpena, and F. Arán-Ais, "Effect of processing time of steam-explosion for the extraction of cellulose fibers from *Phoenix canariensis* palm leaves as potential renewable feedstock for materials," *Polymers*, vol. 14, no. 23, Nov. 2022, Art. no. 5206, doi: 10.3390/polym14235206.

[17] W. Yang, Y. Feng, H. He, and Z. Yang, "Environmentally-friendly extraction of cellulose nanofibers from steam-explosion pretreated sugar beet pulp," *Materials*, vol. 11, no. 7, Jul. 2018, Art. no. 1160, doi: 10.3390/ma11071160.

[18] R. Zhang and Y. Liu, "High energy oxidation and organosolv solubilization for high yield isolation of cellulose nanocrystals (CNC) from Eucalyptus hardwood," *Scientific Reports*, vol. 8, no. 1, Nov. 2018, doi: 10.1038/s41598-018-34667-2.

[19] W. Bessa, D. Trache, A. F. Tarchoun, A. Abdelaziz, M. H. Hussin, and N. Brosse, "Unraveling the effect of kraft and organosolv processes on the physicochemical properties and thermal stability of cellulose and its microcrystals produced from eucalyptus globulus," *Sustainability*, vol. 15, no. 4, Feb. 2023, Art. no. 3384, doi: 10.3390/su15043384.

[20] S. Serna-Loaiza, J. Adamcyk, S. Beisl, M. Miltner, and A. Friedl, "Sequential pretreatment of wheat straw: Liquid hot water followed by organosolv for the production of hemicellulosic sugars, lignin, and a Cellulose-Enriched pulp," *Waste and Biomass Valorization*, vol. 13, no. 12, pp. 4771–4784, Jun. 2022, doi: 10.1007/s12649-022-01824-8.

[21] W. Yu, C. Wang, Y. Yi, H. Wang, L. Zeng, M. Li, Y. Yang, and Z. Tan, "Comparison of deep eutectic solvents on pretreatment of raw ramie fibers for cellulose nanofibril production," *ACS Omega*, vol. 5, no. 10, pp. 5580–5588, Mar. 2020, doi: 10.1021/acsomega.0c00506.

[22] P. V. Barbará, A. A. Rafat, J. P. Hallett, and A. Brandt-Talbot, "Purifying cellulose from major

waste streams using ionic liquids and deep eutectic solvents," *Current Opinion in Green and Sustainable Chemistry*, vol. 41, Jun. 2023, Art. no. 100783, doi: 10.1016/j.cogsc.2023.100783.

[23] L. Douard, J. Bras, T. Encinas, and M. N. Belgacem, "Natural acidic deep eutectic solvent to obtain cellulose nanocrystals using the design of experience approach," *Carbohydrate Polymers*, vol. 252, Jan. 2021, Art. no. 117136, doi: 10.1016/j.carbpol.2020.117136.

[24] V. V. Malolan, C. Trilokesh, K. B. Uppuluri, and A. Arumugam, "Ionic liquid assisted the extraction of cellulose from de-oiled *Calophyllum inophyllum* cake and its characterization," *Biomass Conversion and Biorefinery*, vol. 12, no. 12, pp. 5687–5693, Sep. 2020, doi: 10.1007/s13399-020-01007-2.

[25] W. Rasri, V. T. Thu, A. Corpuz, and L. T. Nguyen, "Preparation and characterization of cellulose nanocrystals from corncob via ionic liquid [Bmim][HSO_4] hydrolysis: Effects of major process conditions on dimensions of the product," *RSC Advances*, vol. 13, no. 28, pp. 19020–19029, Jan. 2023, doi: 10.1039/d3ra02715e.

[26] K. Glińska, J. Gitalt, E. Torrens, N. Plechkova, and C. Bengoa, "Extraction of cellulose from corn stover using designed ionic liquids with improved reusing capabilities," *Process Safety and Environmental Protection*, vol. 147, pp. 181–191, Mar. 2021, doi: 10.1016/j.psep.2020.09.035.

[27] M. S. A. Nurul, D. A. Gopakumar, O. T. F. A., Y. P. Beeran, S. Rizal, N. A. S. Aprilia, D. Hermawan, M. T. Paridah, S. Thomas and A. K. H. P. S., "Extraction of cellulose nanofibers via eco-friendly supercritical carbon dioxide treatment followed by mild acid hydrolysis and the fabrication of cellulose nanopapers," *Polymers*, vol. 11, no. 11, p. 1813, Nov. 2019, doi: 10.3390/polym11111813.

[28] E. L. N. Escobar, T. A. Da Silva, C. L. Pirich, M. L. Corazza, and L. P. Ramos, "Supercritical fluids: a promising technique for biomass pretreatment and fractionation," *Frontiers in Bioengineering and Biotechnology*, vol. 8, Apr. 2020, doi: 10.3389/fbioe.2020.00252.

[29] H. Nasution, E. Yahya, H. A. A. Khalil, M. Shaah, A. Suriani, A. Mohamed, T. Alfatah and C. Abdullah, "Extraction and isolation of cellulose nanofibers from carpet wastes using supercritical carbon dioxide approach," *Polymers*, vol. 11, no. 11, p. 326, Jan. 2022, doi: 10.3390/polym14020326.

[30] R. S. A. Ribeiro, B. C. Pohlmann, V. Calado, N. Bojorge, and N. Pereira, "Production of nanocellulose by enzymatic hydrolysis: Trends and challenges," *Engineering in Life Sciences*, vol. 19, no. 4, pp. 279–291, Feb. 2019, doi: 10.1002/elsc.201800158.

[31] H. Ren, J. Shen, J. Pei, Z. Wang, Z. Peng, S. Fu and Y. Zheng, "Characteristic microcrystalline cellulose extracted by combined acid and enzyme hydrolysis of sweet sorghum," *Cellulose*, vol. 26, pp. 8367–8381, Sep. 2019, doi: 10.1007/s10570-019-02712-6.

[32] D. D. Ribes, A. P. Acosta, D. A. Gatto, E. Piva, R. De Avila Delucis, and R. Beltrame, "Nanofibrillated cellulose extracted by enzymatic hydrolysis followed by mechanical fibrillation," *Journal of Natural Fibers*, vol. 19, no. 14, pp. 9363–9372, Oct. 2021, doi: 10.1080/15440478.2021.1982826.

[33] J. Gröndahl, K. Karisalmi, and J. Vapaavuori, "Micro- and nanocelluloses from non-wood waste sources; processes and use in industrial applications," *Soft Matter*, vol. 17, no. 43, pp. 9842–9858, Jan. 2021, doi: 10.1039/d1sm00958c.

[34] R. S. Abolore, S. Jaiswal, and A. K. Jaiswal, "Green and sustainable pretreatment methods for cellulose extraction from lignocellulosic biomass and its applications: A review," *Carbohydrate Polymer Technologies and Applications*, vol. 7, Nov. 2023, Art. no. 100396, doi: 10.1016/j.carpta.2023.100396.

[35] S. Magalhães, C. Fernandes, J. F. S. Pedrosa, L. Alves, B. Medronho, P. J. T. Ferreira, and M. Da Graça Rasteiro, "Eco-friendly methods for extraction and modification of cellulose: An overview," *Polymers*, vol. 15, no. 14, p. 3138, Jul. 2023, doi: 10.3390/polym15143138.

[36] S. I. Mussatto, G. J. M. Rocha, and I. C. Roberto, "Hydrogen peroxide bleaching of cellulose pulps obtained from brewer's spent grain," *Cellulose*, vol. 15, no. 4, pp. 641–649, Jan. 2008, doi: 10.1007/s10570-008-9198-4.

[37] E. Agboeze, N. P. Ani, and E. O. Omeje, "Extraction and characterization of pharmaceutical grade microcrystalline cellulose from bambara nut (*Voandzeia subterranean* (L) *Thousars*) Husk," *African Scientific Reports*, vol. 1, no. 2, pp. 103–114, Aug. 2022, doi: 10.46481/asr.2022.1.2.31.

[38] F. Kusumattaqiin and W. Chonkaew, "Preparation and characterization of microcrystalline cellulose (MCC) by acid hydrolysis using microwave assisted method from cotton wool," *Macromolecular Symposia*, vol. 354, no. 1, pp. 35–41, Aug. 2015, doi: 10.1002/masy.201400110.

[39] N. D. Kambli, V. Mageshwaran, P. G. Patil, S. Saxena, and R. R. Deshmukh, "Synthesis and characterization of microcrystalline cellulose powder from corn husk fibres using bio-chemical route," *Cellulose*, vol. 24, no. 12, pp. 5355–5369, Oct. 2017, doi: 10.1007/s10570-017-1522-4.

[40] Z. Ahmad, N. N. Roziaizan, R. Rahman, A. F. Mohamad, and W. I. N. W. Ismail, "Isolation and characterization of microcrystalline cellulose (MCC) from rice husk (RH)," *MATEC Web of Conferences*, vol. 47, Apr. 2016, Art. no. 05013, doi: 10.1051/matecconf/20164705013.

[41] A. S. N. Hanani, A. Zuliahani, W. I. Nawawi, N. Razif, and A. R. Rozyanty, "The effect of various acids on properties of microcrystalline cellulose (MCC) extracted from rice husk (RH)," *IOP Conference Series: Materials Science and Engineering*, vol. 204, Apr. 2017, Art. no. 012025, doi: 10.1088/1757-899x/204/1/012025.

[42] H. Chen, "Lignocellulose biorefinery feedstock engineering," in *Lignocellulose Biorefinery Engineering*, Amsterdam, Netherlands: Elsevier, pp. 37–86, 2015, doi: 10.1016/b978-0-08-100135-6.00003-x.

[43] F. Fitriani, S. Aprilia, N. Arahman, and M. R. Bilad, "Effect of acid concentration on the properties of microcrystalline cellulose from pineapple crown leaf," *Jurnal Rekayasa Kimia & Lingkungan*, vol. 17, no. 1, pp. 1–7, 2022, doi: 10.23955/rkl.v17i1.21010.

[44] M. Z. Karim, Z. Z. Chowdhury, S. B. A. Hamid, and M. E. Ali, "Statistical optimization for acid hydrolysis of microcrystalline cellulose and its physiochemical characterization by using metal ion catalyst," *Materials*, vol. 7, no. 10, pp. 6982–6999, Oct. 2014, doi: 10.3390/ma7106982.

[45] F. Fitrya, N. A. Fithri, and D. P. Wijaya, "Optimization of acid concentration and hydrolysis time in the isolation of microcrystalline cellulose from water hyacinth (*Eichornia crassipes solm*)," *Tropical Journal of Natural Product Research (TJNPR)*, vol. 5, no. 3, pp. 503–508, Apr. 2021, doi: 10.26538/tjnpr/v5i3.14.

[46] K. M. Vanhatalo and O. P. Dahl, "Effect of mild acid hydrolysis parameters on properties of microcrystalline cellulose," *BioResources*, vol. 9, no. 3, pp. 4729–4740, May 2014, doi: 10.15376/biores.9.3.4729-4740.

[47] W. T. N. Boschetti, A. M. M. L. Carvalho, A. De Cássia Oliveira Carneiro, G. B. Vidaurre, F. J. B. Gomes, and D. N. Soratto, "Effect of mechanical treatment of eucalyptus pulp on the production of nanocrystalline and microcrystalline cellulose," *Sustainability*, vol. 13, no. 11, p. 5888, May 2021, doi: 10.3390/su13115888.

[48] M. Asif, D. Ahmed, N. Ahmad, M. T. Qamar, N. K. Alruwaili, and S. N. A. Bukhari, "Extraction and characterization of microcrystalline cellulose from *Lagenaria siceraria* fruit pedicles," *Polymers*, vol. 14, no. 9, p. 1867, May 2022, doi: 10.3390/polym14091867.

[49] R. Javier-Astete, J. Jimenez-Davalos, and G. Zolla, "Determination of hemicellulose, cellulose, holocellulose and lignin content using FTIR in *Calycophyllum spruceanum* (Benth.) K. Schum. and *Guazuma crinita* Lam.," *PLoS ONE*, vol. 16, no. 10, Oct. 2021, Art. no. e0256559, doi: 10.1371/journal.pone.0256559.

[50] M. J. Pancholi, A. Khristi, A. K. M., and D. Bagchi, "Comparative analysis of lignocellulose agricultural waste and pre-treatment conditions with ftir and machine learning modeling," *BioEnergy Research*, vol. 16, no. 1, pp. 123–137, Apr. 2022, doi: 10.1007/s12155-022-10444-y.

[51] M. P. Gundupalli, P. Tantayotai, E. J. Panakkal, S. Chuetor, S. Kirdponpattara, A. S. S. Thomas, B. K. Sharma, and M. Sriariyanun, "Hydrothermal pretreatment optimization and deep eutectic solvent pretreatment of lignocellulosic biomass: An integrated approach," *Bioresource Technology Reports*, vol. 17, Feb. 2022, Art. no. 100957, doi: 10.1016/j.biteb.2022.100957.

[52] F. Xu, J. Yu, T. Tesso, F. Dowell, and D. Wang, "Qualitative and quantitative analysis of lignocellulosic biomass using infrared techniques: A mini-review," *Applied Energy*, vol. 104, pp. 801–809, Apr. 2013, doi: 10.1016/j.apenergy.2012.12.019.

[53] Z. Deng, A. Xia, Q. Liao, X. Zhu, Y. Huang, and Q. Fu, "Laccase pretreatment of wheat straw: effects of the physicochemical characteristics and the kinetics of enzymatic hydrolysis," *Biotechnology for Biofuels*, vol. 12, no. 1, Jun. 2019, doi: 10.1186/s13068-019-1499-3.

[54] M. Woźniak, I. Ratajczak, D. Wojcieszak, A. Waśkiewicz, K. Szentner, J. Przybył, S. Borysiak, and P. Goliński, "Chemical and structural characterization of maize stover fractions in aspect of its possible applications," *Materials*, vol. 14, no. 6, p. 1527, Mar. 2021, doi: 10.3390/ma14061527.

[55] J. S. Lupoi, E. Gjersing, and M. F. Davis, "Evaluating lignocellulosic biomass, its derivatives, and downstream products with raman spectroscopy," *Frontiers in Bioengineering and Biotechnology*, vol. 3, Apr. 2015, doi: 10.3389/fbioe.2015.00050.

[56] M. K. M. Haafiz, S. J. Eichhorn, A. Hassan, and M. Jawaid, "Isolation and characterization of microcrystalline cellulose from oil palm biomass residue," *Carbohydrate Polymers*, vol. 93, no. 2, pp. 628–634, Apr. 2013, doi: 10.1016/j.carbpol.2013.01.035.

[57] R. Ravindran, S. Jaiswal, N. Abu-Ghannam, and A. K. Jaiswal, "A comparative analysis of pretreatment strategies on the properties and hydrolysis of brewers' spent grain," *Bioresource Technology*, vol. 248, pp. 272–279, Jan. 2018, doi: 10.1016/j.biortech.2017.06.039.

[58] V. Kumar and S. H. Kothari, "Effect of compressional force on the crystallinity of directly compressible cellulose excipients," *International Journal of Pharmaceutics*, vol. 177, no. 2, pp. 173–182, Jan. 1999, doi: 10.1016/s0378-5173(98)00340-8.

[59] N. A. Heidari, M. Fathi, N. Hamdami, H. Taheri, G. Siqueira, and G. Nyström, "Thermally insulating cellulose nanofiber aerogels from brewery residues," *ACS Sustainable Chemistry & Engineering*, vol. 11, no. 29, pp. 10698–10708, Jul. 2023, doi: 10.1021/acssuschemeng.3c01113.

[60] L. Camacho-Núñez, S. Jurado-Contreras, M. D. La Rubia, F. J. Navas-Martos, and J. A. Rodríguez-Liébana, "Cellulose-based upcycling of Brewer´s spent grains: Extraction and acetylation," *Journal of Polymers and the Environment*, vol. 32, pp. 1–14, Dec. 2023, doi: 10.1007/s10924-023-03137-w.

[61] K. Bhandari, S. R. Maulik, and A. R. Bhattacharyya, "Synthesis and characterization of microcrystalline cellulose from rice husk," *Journal of the Institution of Engineers (India) Series E*, vol. 101, no. 2, pp. 99–108, Mar. 2020, doi: 10.1007/s40034-020-00160-7.